

# Model Reference Adaptive Control of SPS-Based Dual Active Bridge Converter with Constant Power Loading

Research paper

Emmanuel K. Effah<sup>1,2,\*</sup>, Emmanuel K. Anto<sup>3</sup>, Philip Y. Okyere<sup>3</sup>, Francis B. Effah<sup>3</sup>

<sup>1</sup>Department of Electrical/Electronic Engineering, Kwame Nkrumah University of Science and Technology, Kumasi, Ghana

<sup>2</sup>Department of Electrical/Electronic Engineering, Ghana Communication Technology University, Accra, Ghana

<sup>3</sup>Department of Electrical/Electronic Engineering, Kwame Nkrumah University of Science and Technology, Kumasi, Ghana

Received: 14 February 2024; Accepted: 23 May 2024

**Abstract:** This paper presents a new model reference adaptive-based control (MRAC) for a single-phase shift-modulated dual active bridge DC-DC converter (SPS-DAB) with constant power loading (CPL). The non-linear control algorithm, developed based on the reduced order model of the converter, is subjected to a thorough stability and convergence analysis. The efficacy of the proposed control strategy is verified through simulations conducted on MATLAB R2023a and PLECS 4.5.6, demonstrating its capability to counteract the destabilising effects of the CPL, while ensuring precise tracking of the dual active bridge (DAB) output voltage, even amidst parameter variations. Comparative analysis highlights the superior robustness and performance of the proposed approach over the conventional proportional-integral (PI) controllers.

**Keywords:** dual active bridge converter • model reference adaptive control • multi-converter power systems • constant power loads

## 1. Introduction

The DC microgrid has gained attention recently, and it is set to be indispensable in future power systems due to the strong advocacy for the high penetration of renewable energy sources (Zhang et al., 2020). DC microgrids present substantial benefits such as higher efficiency and improved current capacity compared to traditional AC systems. They ensure improved reliability and controllability and are exempt from challenges of frequency synchronisation (Dragičević et al., 2016; Hossain et al., 2018; Shao et al., 2022).

The general architecture of the DC microgrid contains power converters cascaded to supply energy from the source to the DC bus and another set of cascaded converters providing energy to the loads from the DC bus (Dragičević et al., 2016; Lucas et al., 2020). This structure is usually termed a multi-converter power system. Again, many loads connected to the DC microgrid, such as motor drives and electric vehicles are tightly regulated. Multi-converter systems and tightly regulated loads exhibit constant power loading (CPL) characteristics (Lucas et al., 2020). This means that the DC microgrids exhibit negative incremental resistance, adversely affecting the system's damping properties. This makes the issue of instability caused by the same a significant concern.

Researchers have made significant contributions to tackling this issue. The concept of adding extra equipment to improve damping or ensuring constraints of input impedances has been investigated (AL-Nussairi et al., 2017; Rahimi and Emadi, 2009). While this method is simple and effective, it increases system losses and costs.

\* Email: ekeffamp@gmail.com

Therefore, many control strategies, both linear and non-linear, have been investigated to manipulate the duty cycle of power converters to achieve the same goal without sacrificing efficiency (Csizmadia and Kuczmann, 2022). Linear controllers such as the linear active stabilising (Radwan and Mohamed, 2012), proportional compensator (Liutanakul et al., 2010), power shaping stabilisation control (Wang and Howe, 2008) and the virtual resistance (Wu and Lu, 2015) have been developed. These strategies are based on the small signal analysis of the system where its design and performance are about a stable local point. Hence, performance deteriorates when the model deviates from the actual system parameters or in the event of a large signal disturbance. Non-linear control measures have been widely deployed to ensure stabilisation and control. Approaches such as sliding mode control and backstepping control methods have been variedly applied to ensure stability and good tracking (Meng et al., 2023; Singh et al., 2015; Wu and Lu, 2019). While sliding mode control grapples with the chattering issue of its output, backstepping requires that the model be presented in a strict form. Besides, backstepping depends very much on the accuracy of the model. Backstepping combined with the Kalman filter to improve its robustness has been reported by Yousefizadeh et al. (2019), but it must be manually adjusted. The model reference adaptive control has also been reported in the literature (Brando et al., 2018; Veeramraju et al., 2022); however, analyses were done based on resistive loads.

Nevertheless, there is no general solution to the problem, and more research needs to be done in this field. Again, most of the above control strategies were implemented on the traditional DC-DC power converter.

The dual active bridge (DAB) is one of the most promising isolated bidirectional DC/DC power converter topologies for microgrid applications (Do et al., 2024; Shao et al., 2022). It, therefore, needs to be evaluated to verify its performance in a challenging situation as being subjected to CPL. Considering the MRAC-based ability to ensure good performance amid parameter variation or large disturbance (Hajji et al., 2020; Zorgani et al., 2019), this paper seeks to apply MRAC on DAB with CPL. It proposes a new control strategy based on direct model reference adaptive control to overcome the destabilising effect of the constant power load as well as ensuring good tracking of the output voltage of the DAB. Additionally, the stability and convergence analysis from the theoretical perspective has been provided for a step-by-step appreciation of the algorithm. Results show that the MRAC-based algorithm can overcome the destabilising effect of the CPL while providing better performance compared to the traditional controllers when subjected to large disturbances and parameter variations.

The rest of the paper is summarised as follows: Section 2 deals with the modelling of a DAB converter with CPL, Section 3 provides the stability, convergence, and control analysis of the model reference adaptive control of the DAB with CPL. Section 4 provides the results and discussion of simulations undertaken in MATLAB and PLECS.

## 2. Modelling of a DAB with CPL

Modelling plays a crucial role in devising effective control strategies for diverse physical systems. Existing literature outlines various modelling approaches for power converters, including the reduced order model, generalised state space average model approach, and discrete-time model (Mueller and Kimball, 2018; Iqbal et al., 2020; Shah and Bhattacharya, 2017). A thorough comparison of these approaches, considering factors such as complexity and accuracy under both small and large disturbances, has established that the reduced order model of the DAB stands out as the most optimal choice (He et al., 2023; Shao et al., 2022). Consequently, the DAB with CPL is developed based on the reduced order approach. Additionally, the single-phase shift (SPS) modulation technique is selected due to its broader scope of implementation and application in today's industry when compared to other advanced modulation techniques (He et al., 2023).

Figure 1 shows the general topology of the SPS-based DAB, connected to a load resistor and a constant power load.  $v_1$ ,  $i_{b1}$ ,  $v_2$  and  $i_{b2}$  are the input voltage, input current, output voltage, and output current of the DAB, respectively.  $C_1$  and  $C_2$  are the input and output capacitances of the DAB.  $N$  is the primary to secondary turns ratio of the high-frequency isolated transformer.  $S_x$  (where  $x = 1-8$ ) represent the active switches, typically an insulated gate bipolar transistor (IGBT). These switches are connected to the antiparallel diode as shown in Figure 1. The active switches are provided with the control signal to produce voltages  $v_{ab}$  and  $v_{cd}$ . In the production of voltage  $v_{ab}$  at the primary side of the high frequency transformer, the control signals of the pair S1 and S4 must be identical and that of S2 and S3 must also be identical. However, the two pairs must be complementary 50% duty cycle signals. At the secondary

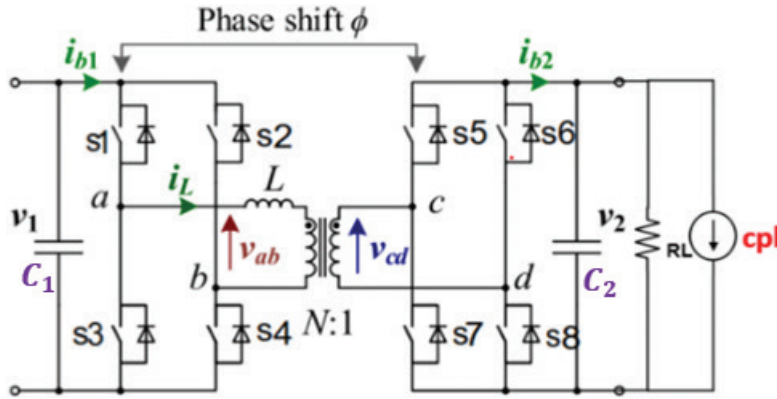


**Figure 1.** Topology of DAB connected with CPL load. CPL, constant power loading; DAB, dual active bridge.

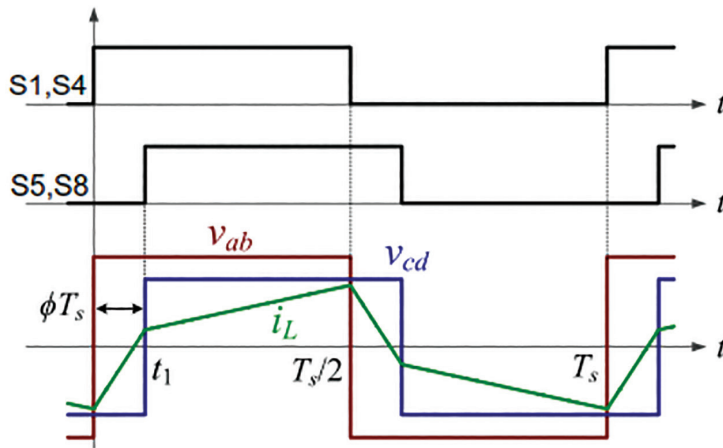


**Figure 2.** SPS modulation and associated current and voltage. SPS, single-phase shift.

side of the transformer,  $v_{cd}$  is produced using a similar approach: The pair (S5, S8) is subjected to the same control signal of 50% duty cycle and the pair (S6, S7) is subjected to another control signal, which is complementary to that of the pair (S5, S8). The control signals of the secondary bridge replicate those of the primary bridge, albeit with a phase shift  $\phi$ . Therefore,  $v_{ab}$  and  $v_{cd}$  can have only two states (positive and negative) as shown in Figure 2. The voltage waveforms shown in Figure 2, the rectified inductor current waveform and the principle that the rate of change of inductor current is proportional to the ratio of the total voltage across it to its inductance ( $\frac{di_L}{dt} = \frac{v_L}{L}$ ) can then be used to derive the output power. The average output current from the DAB,  $\langle i_{b2} \rangle$ , is then determined and used for onward analysis with the rest of the circuit components. The output current and the input current waveforms have been shown in Figure 3. Analysis of half of the period suffices as the DAB has symmetric characteristics.

Considering the power equation in Qin and Kimball (2012) and referring it from the secondary to the primary side of the high-frequency transformer, the output power equation can be expressed as

$$P_{out} = \frac{Nv_1v_2d(1-d)}{2f_sL} \quad (1)$$

$$d = \frac{2\phi}{T_s} \quad (2)$$

$P_{out}$  = output power,  $N$  = turns ratio of the transformer,  $f_s$  = switching frequency of DAB,  $d$  = phase shift ratio as expressed in Eq. (2).

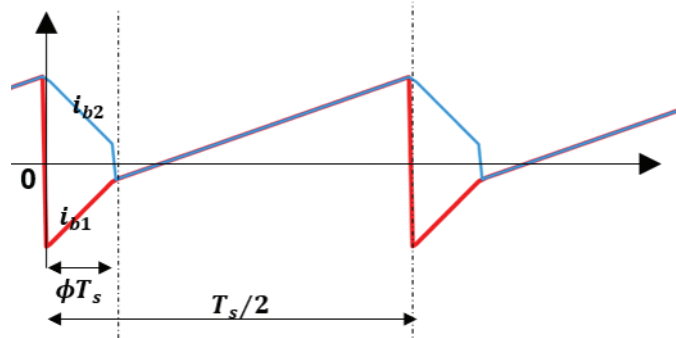


**Figure 3.** Input and output current waveforms.

$\langle i_{b2} \rangle$  is determined from  $P_{out}$ . This is achieved by making  $\langle i_{b2} \rangle$  the subject of the equation  $P_{out} = v_2 \langle i_{b2} \rangle$ . This value is subsequently used to obtain the model of the DAB.

At the output end, the DAB is connected to the load resistor representing a constant voltage source and the CPL. The voltage current characteristics of the CPL is expressed as  $i_{cpl} = \frac{P_{cpl}}{v_2}$ , where  $P_{cpl}$  is the constant power demanded by the load. This equation is adopted in the analysis as opposed to that of the linearised equation of the CPL, to cater for large disturbances. Using the Kirchhoff's current law at the output end of the DAB and choosing  $v_2$  as a state variable, the state equation of the reduced order DAB model is finally given by:

$$\frac{dv_2}{dt} = \frac{-v_2}{R_L C_2} - \frac{P_{cpl}}{C_2 v_2} + \frac{Nv_1 d(1-d)}{2f_s LC_2} \quad (3)$$

### 3. Design of Model Reference Adaptive Control

The direct model reference adaptive control is adopted in this analysis. Considering that the model developed in Section 2 is a first-order system, the reference model with the desired dynamics ( $a_m < 0$ ) can be designed as;

$$\dot{y}_m = a_m y_m + k_m r \quad (4)$$

The DAB model can also be written as

$$\dot{y}_s = a_s y_s + f(y_s) + k_s u \quad (5)$$

with

$$y_s = v_2, k_s = \frac{Nv_1}{2f_s LC_2}, f(y_s) = -\frac{P_{cpl}}{C_2 v_2}, a_s = \frac{-1}{R_L C_2} \text{ and } u = d(1-d)$$

With the objective of having the actual output of the DAB ( $y_s$ ) track the output of the reference model ( $y_m$ ), let the tracking error,  $e = y_s - y_m$ . Then the ideal controller  $u^*$ , given in Eq. (6), would ensure zero tracking error. In Eq. (6), it is assumed that the parameters ( $w_r, w_y, w_d$ ) are constant. The parameters are further expressed as shown in Eqs. (7)–(9).

$$u^* = w_r r + w_y y_s - w_d \quad (6)$$

$$w_y = \frac{a_m y_m - a_s y_s}{k_s} \quad (7)$$

$$w_r = \frac{k_m}{k_s} \quad (8)$$

$$w_d = \frac{f(y_s)}{k_s} \quad (9)$$

However, these controller parameters are unknown hence can be represented as

$$u = \hat{w}_r r + \hat{w}_y y_s - \hat{w}_d \quad (10)$$

The adjustment of these parameters would be performed in real-time by utilising the data accessible from the control system. Considering the aforementioned equations, the reference model and the DAB model can be reformulated as follows:

$$\dot{y}_m = a_s y_m + k_s (w_y y_m + w_r r) \quad (11)$$

$$\dot{y}_s = a_s y_s + f(y_s) + k_s (\hat{w}_r r + \hat{w}_y y_s - \hat{w}_d) \quad (12)$$

The tracking equation can then be expressed as

$$\begin{aligned} \dot{e} &= \dot{y}_s - \dot{y}_m \\ &= a_s e + f(y_s) + k_s ((\hat{w}_r - w_r) r + \hat{w}_y y_s - w_y y_m - \hat{w}_d) \\ &= a_s e + f(y_s) + k_s ((\hat{w}_r - w_r) r + \hat{w}_y y_s - w_y y_s + w_y y_s - w_y y_m - \hat{w}_d) \\ &= a_s e + f(y_s) - \hat{w}_d + k_s \tilde{w}_r r + k_s (\tilde{w}_y y_s + w_y e) \\ &= a_m e + k_s (\tilde{w}_r r + \tilde{w}_y y_s) - \tilde{w}_d \end{aligned} \quad (13)$$

Noting that  $f(y_s) - \hat{w}_d = -\tilde{w}_d$ ,  $\hat{w}_r - w_r = \tilde{w}_r$  and  $\hat{w}_y - w_y = \tilde{w}_y$

Choosing Lyapunov equation as

$$\dot{V}(e, \tilde{w}_y, \tilde{w}_r, \tilde{w}_d) = \frac{e\dot{e}}{k_s} + \frac{\tilde{w}_y \dot{\tilde{w}}_y}{\gamma_y} + \frac{\tilde{w}_r \dot{\tilde{w}}_r}{\gamma_r} + \frac{\tilde{w}_d \dot{\tilde{w}}_d}{\gamma_d} \quad (14)$$

$$\begin{aligned} \dot{V}(e, \tilde{w}_y, \tilde{w}_r, \tilde{w}_d) &= \frac{1}{k_s} e (a_m e + k_s (\tilde{w}_r r + \tilde{w}_y y_s) - \tilde{w}_d) + \frac{\tilde{w}_y \dot{\tilde{w}}_y}{\gamma_y} + \frac{\tilde{w}_r \dot{\tilde{w}}_r}{\gamma_r} + \frac{\tilde{w}_d \dot{\tilde{w}}_d}{\gamma_d} \\ &= \frac{a_m e^2}{k_s} \end{aligned} \quad (15)$$

From this, it can be realised that setting adaptation laws as in Eqs (16)–(18), it ensures that  $\dot{V}(e, \tilde{w}_y, \tilde{w}_r, \tilde{w}_d) \leq 0$  and hence all parameters are bounded.

$$\dot{\tilde{w}}_y = -\gamma_y e y_s \quad (16)$$

$$\dot{\tilde{w}}_r = -e \gamma_r r \quad (17)$$

$$\dot{\tilde{w}}_d = -e \gamma_d \quad (18)$$

To verify that the tracking error converges to zero, the Barbalat's lemma is adopted. The first condition  $V(e, \tilde{w}_y, \tilde{w}_r, \tilde{w}_d)$  must have a finite limit at  $t \rightarrow \infty$ . Since  $\dot{V}(e, \tilde{w}_y, \tilde{w}_r, \tilde{w}_d) \leq 0$ , then

$$\begin{aligned} V(e(t \rightarrow \infty), \tilde{w}_y(t \rightarrow \infty), \tilde{w}_r(t \rightarrow \infty), \tilde{w}_d(t \rightarrow \infty)) &= V(e(0), \tilde{w}_y(0), \tilde{w}_r(0), \tilde{w}_d(0)) - \int_0^{\infty} \dot{V}(e, \tilde{w}_y, \tilde{w}_r, \tilde{w}_d) dt \\ &= V(e(0), \tilde{w}_y(0), \tilde{w}_r(0), \tilde{w}_d(0)) + \frac{a_m}{k_s} \|e\|_b^2 < \infty \end{aligned} \quad (19)$$

Hence, the first condition is satisfied.

Next,  $\dot{V}(e, \tilde{w}_y, \tilde{w}_r, \tilde{w}_d)$  must be shown to be uniformly continuous. The derivative of this function must exist to satisfy this condition.

$\dot{V} = \frac{2}{k_s} a_m e (a_m e + k_s (\tilde{w}_r r + \tilde{w}_y y_s) - \tilde{w}_d)$ ; as it has been previously established that all these parameters are bounded, this makes the given equation also bounded, hence satisfying this condition. Barbalat's lemma is therefore satisfied and hence the tracking error,  $e$ , is asymptotically stable.

## 4. Simulation Results

To verify the theory above, a simulation was conducted in MATLAB and a further circuit simulation analysis conducted in PLECS. The parameters used are provided in Table 1.

The CPL was inculcated into the algorithm in its generic form that is  $i_{cpl} = \frac{P_{cpl}}{v_2}$ . This was done to extend the range of analysis beyond the operating point (Rahimi et al., 2010). To ensure that CPL could work in PLECS, a C-Script was developed to feed a variable resistor as a model for the CPL. To avoid running into errors (NaN), a limit was established in the C-Script to take care of infinite conditions when the voltage was zero. This is consistent with literature (Leonard, 2014), where in real power, electronic converters either include a lock feature, which disables operation below a specific input voltage or a protective fuse is included to protect the internal parts from overcurrent.

Results of the control of DAB system with CPL using MRAC from MATLAB is as shown in Figures 4 and 5. Figure 4 shows results considering an adaptive gain of 0.002 and Figure 5 shows results when the adaptive gain is 0.02. Using the MRAC, the output voltage ( $y_s$ ) tracks the output of the reference model ( $y_m$ ) following minor disturbances caused by parameter changes (at time 0.03 s,  $v_1$  was changed from 400 V to 450 V) and large disturbances (at time 0.09 s, output voltage changed from 160 V to 50 V, while  $v_1 = 450$  V). The transient responses follow that of the reference model when minor disturbances are recorded.

Results also indicate the convergence of the estimated adaptive parameters ( $w_r, w_y$ ). Again, results show that the adaptive gain impacts the system responses. Generally, small adaptive gains were recorded for the control system. It was also noticed that the smaller the adaptive gain, the less rigorous the control action ( $u(t)$ ) and the greater the drift from the model transient response. For example, considering the time interval from 90 ms to 94 ms in Figures 4 and 5, an increase in the adaptive gain by a factor of ten leads to a proportional increase in the speed of the control action by a factor of three. However, as can be observed, this action improves the tracking of the output voltage transients with respect to the reference model output. This means that although increasing the adaptive gain would better track both the transient and steady-state output voltages, care must be taken not to outwork the control input

**Table 1.** Parameters used in simulation.

Symbol	Parameter	Units	Values
$f_s$	Switching frequency	kHz	20
$L$	Inductance	$\mu$ H	70
$N$	Transformer turns ratio		2:1
$C_2$	DC capacitor at the output	mF	1
$R_L$	Load resistor	$\Omega$	4

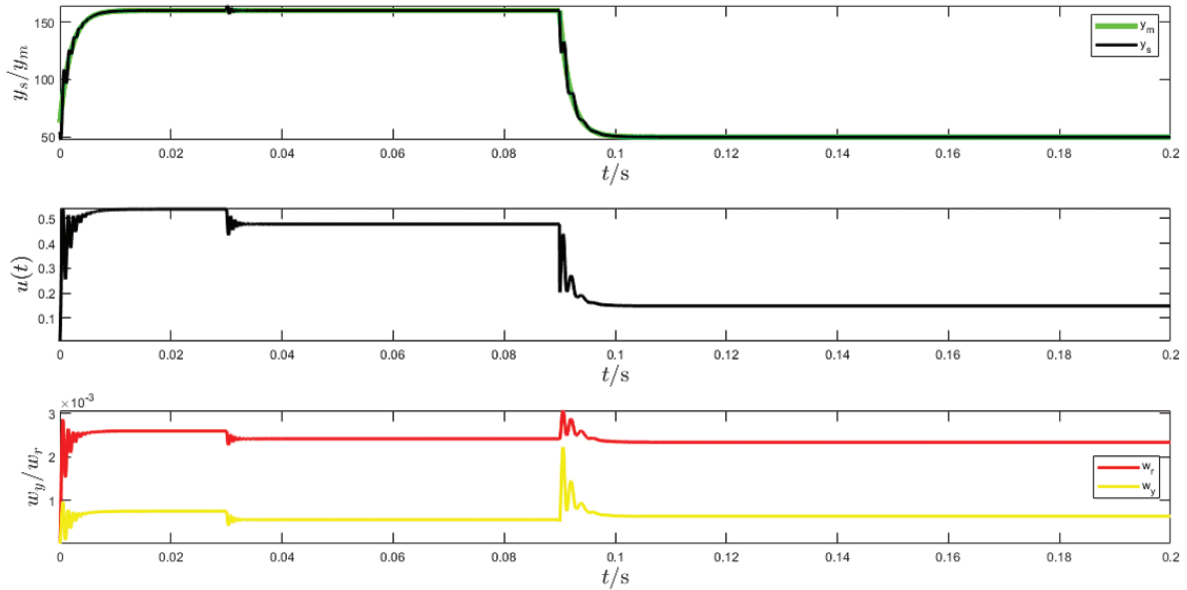


**Figure 4.** DAB system responses to small and large disturbances when adaptive gains = 0.002. DAB, dual active bridge.

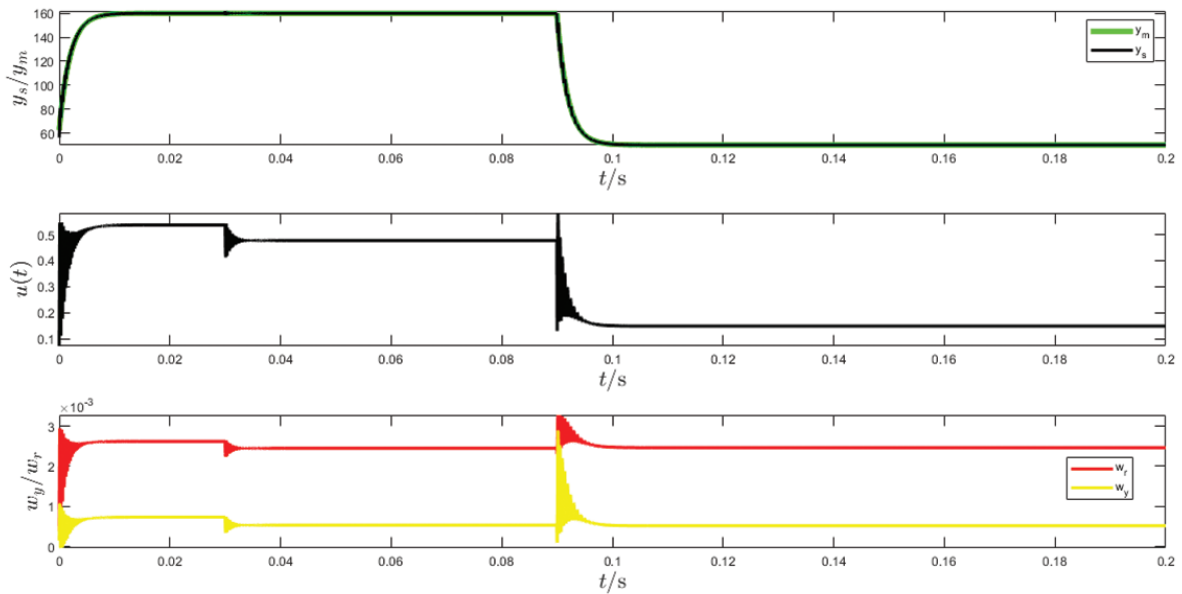


**Figure 5.** DAB system responses to small and large disturbances when adaptive gains = 0.02. DAB, dual active bridge.

overly. Hence, there may be a trade-off between the performance of output voltage and the constraints placed on the control input.

To assess the performance of the MRAC strategy, its results were compared with that of the traditional (and often used) proportional-integral (PI) controller in terms of output voltage tracking. Simulation results from PLECS demonstrating general superiority of MRAC in tracking the output voltage of the DAB with CPL is shown in Figure 6. Initially, the MRAC-controlled DAB exhibited deviations from the desired voltage of 160 V, as observed from the oscillations between zero and 30 ms, with a maximum deviation of 14 V. The deviations are attributed to the learning phase of the adaptive controller. However, this condition persisted for a short duration of 25 ms, after which the steady-state performance of the MRAC surpassed that of the PI controller. This is evident in the final output voltage

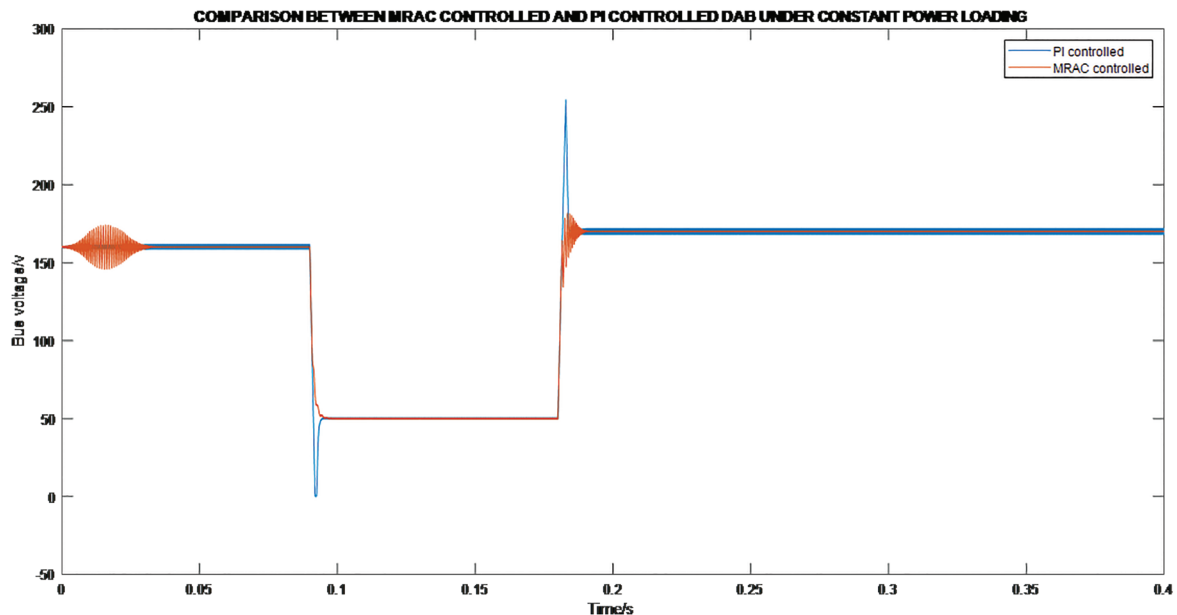


**Figure 6.** PLECS results for comparison between MRAC controlled and PI controlled DAB with CPL. CPL, constant power loading; DAB, dual active bridge; PI, proportional-integral.

of the MRAC ranging from 159.9 V to 160.2 V compared to the PI controlled with voltages ranging from 158.5 V to 161.8 V. Again, at the CPL requiring lower voltage ( $v_2 = 50$  V), PI controller causes the voltage to dip to almost zero volts indicating instability. However, the MRAC has the ability to learn the output disturbance quickly, and hence adequately tracks the output voltage. At 170 V, even though transients of the output of the MRAC controlled system are initially oscillatory, its peak overshoot is not as high as that of the output of the traditional controlled system.

## 5. Conclusion

In this paper, a new model reference adaptive based control (MRAC) has been developed for the control of a DAB bidirectional DC-DC converter with CPL. The proposed non-linear control was formulated based on the reduced order model of DAB, given the good results it provides with resistive loads. Additionally, the stability and convergence analysis from the theoretical perspective has been provided for a step-by-step appreciation of the algorithm.

Simulation results show that the new control strategy can overcome the destabilising effect of the constant power load as well as ensuring good tracking of the output voltage of the DAB in the midst of large disturbances and parameter variation. Again, a comparative analysis of results shows that the MRAC-based algorithm provides better performance compared to the traditional PI controllers when subjected to large disturbances.

## References

- AL-Nussairi, M. K., Bayindir, R., Padmanaban, S., Mihet-Popa, L. and Siano, P. (2017). Constant Power Loads (CPL) with Microgrids: Problem Definition, Stability Analysis and Compensation Techniques. *Energies*, 10(10), p. 1656. doi: 10.3390/en10101656.
- Brando, G., Del Pizzo, A. and Meo, S. (2018). Model-reference adaptive control of a dual active bridge DC-DC converter for aircraft applications. In: *SPEEDAM 2018 - Proceedings: International Symposium on Power Electronics, Electrical Drives, Automation and Motion*, 20–22 June 2018, Amalfi, Italy: IEEE, pp. 502–506. doi: 10.1109/SPEEDAM.2018.8445242.
- Csizmadia, M. and Kuczmann, M. (2022). Extended Feedback Linearisation Control of Non-ideal DCDC

- Buck Converter in Continuous-conduction Mode, *Power Electronics and Drives*, 7(42), pp. 1–8. doi: 10.2478/pead-2022-0001.
- Do, T. A., Nguyen, Q. D. and Vu, P. (2024). Design and Implementation of a Current-FED Dual Active Bridge Converter for an AC Battery. *Journal of Electrical Engineering*, 75(1), pp. 47–55. doi: 10.2478/jee-2024-0007.
- Dragičević, T., Lu, X., Vasquez, J. C. and Guerrero, J. M. (2016). DC Microgrids – Part I: A Review of Control Strategies and Stabilization Techniques. *IEEE Transactions on Power Electronics*, 31(7), pp. 4876–4891. doi: 10.1109/TPEL.2015.2478859.
- Hajji, S., Zayani, H., Bouaziz, N. and Ben Chehida, R. (2020). Sensorless Induction Motor Drive Based on Model Reference Adaptive System Scheme Utilising a Fictitious Resistance. *Power Electronics and Drives*, 5(41), pp. 199–213. doi: 10.2478/pead-2020-0015.
- He, J., Chen, Y., Lin, J., Chen, J., Cheng, L. and Wang, Y. (2023). Review of Modeling, Modulation, and Control Strategies for the Dual-Active-Bridge DC/DC Converter. *Energies*, 16(18), p. 6646. doi: 10.3390/en16186646.
- Hossain, M. Z., Rahim, N. A. and Selvaraj, J. (2018). Recent Progress and Development on Power DC-DC Converter Topology, Control, Design and Applications: A Review. *Renewable and Sustainable Energy Reviews*, 81(Part 1), pp. 205–230. doi: 10.1016/j.rser.2017.07.017.
- Iqbal, M. T., Maswood, A. I., Dehghani Tafti, H., Tariq, M. and Bingchen, Z. (2020). Explicit Discrete Modelling of Bidirectional Dual Active Bridge DC-DC Converter using Multi-Time Scale Mixed System Model. *IET Power Electronics*, 13(18), pp. 4252–4260. doi: 10.1049/iet-pel.2020.0293.
- Leonard, J. P. (2014). Nonlinear Modeling of DC Constant Power Loads with Frequency Domain Volterra Kernels. Available at: <https://diginole.lib.fsu.edu/islandora/object/fsu%3A252857>.
- Liutanakul, P., Awan, A. and Pierfederici, S. (2010). Linear Stabilization of a DC Bus Supplying a Constant Power Load: A General Design Approach. *IEEE Transactions on Power Electronics*, 25(2), pp. 475–488. doi: 10.1109/TPEL.2009.2025274.
- Lucas, K. E., Pagano, D. J., Plaza, D. A., Vaca-Benavides, D. A. and Ríos, S. J. (2020). Robust Feedback Linearization Control for DAB Converter Feeding a CPL. *IFAC-PapersOnLine*, 53(2), pp. 13402–13409. doi: 10.1016/j.ifacol.2020.12.178.
- Meng, X., Jia, Y., Xu, Q., Ren, C., Han, X. and Wang, P. (2023). A Novel Intelligent Nonlinear Controller for Dual Active Bridge Converter with Constant Power Loads. *IEEE Transactions on Industrial Electronics*, 70(3), pp. 2887–2896. doi: 10.1109/TIE.2022.3170608.
- Mueller, J. A. and Kimball, J. W. (2018). An Improved Generalized Average Model of DC-DC Dual Active Bridge Converters. *IEEE Transactions on Power Electronics*, 33(11), pp. 9975–9988. doi: 10.1109/TPEL.2018.2797966.
- Qin, H. and Kimball, J. W. (2012). Generalized Average Modeling of Dual Active BRIDGE DC-DC Converter. *IEEE Transactions on Power Electronics*, 27(4), pp. 2078–2084. doi: 10.1109/TPEL.2011.2165734.
- Radwan, A. A. A. and Mohamed, Y. A. R. I. (2012). Linear Active Stabilization of Converter-Dominated DC Microgrids. *IEEE Transactions on Smart Grid*, 3(1), pp. 203–216. doi: 10.1109/TSG.2011.2162430.
- Rahimi, A. M., Williamson, G. A. and Emadi, A. (2010). Loop-Cancellation Technique: A Novel Nonlinear Feedback to Overcome the Destabilizing Effect of Constant-Power Loads. *IEEE Transactions on Vehicular Technology*, 59(2), pp. 650–661. doi: 10.1109/TVT.2009.2037429.
- Rahimi, A. M. and Emadi, A. (2009). Active Damping in DC/DC Power Electronic Converters: A Novel Method to Overcome the Problems of Constant Power Loads. *IEEE Transactions on Industrial Electronics*, 56(5), pp. 1428–1439. doi: 10.1109/TIE.2009.2013748.
- Shah, S. S. and Bhattacharya, S. (2017). Large & small signal modeling of dual active bridge converter using improved first harmonic approximation. In: *Conference Proceedings - IEEE Applied Power Electronics Conference and Exposition (APEC)*, 26–30 March 2017, Tampa, FL, USA: IEEE, pp. 1175–1182. doi: 10.1109/APEC.2017.7930844.
- Shao, S., Chen, L., Shan, Z., Gao, F., Chen, H., Sha, D. and Dragičević, T. (2022). Modeling and Advanced Control of Dual-Active-Bridge DC-DC Converters: A Review. *IEEE Transactions on Power Electronics*, 37(2), pp. 1524–1547. doi: 10.1109/TPEL.2021.3108157.
- Singh, S., Fulwani, D. and Kumar, V. (2015). Robust Sliding-Mode Control of DC/DC Boost Converter Feeding a Constant Power Load. *IET Power Electronics*, 8(7), pp. 1230–1237. doi: 10.1049/IET-PEL.2014.0534.
- Veeramraju, K. J. P., Cardoza, A., Sarangapani, J. and Kimball, J. W. (2022). Robust modifications to model reference adaptive control for reference voltage tracking in a dual active bridge DC-DC converter. In: *2022 IEEE Energy Conversion Congress and Exposition (ECCE)*, 09–13 October

- 2022, Detroit, MI, USA: IEEE. doi: 10.1109/ECCE50734.2022.9947779.
- Wang, J. and Howe, D. (2008). A Power Shaping Stabilizing Control Strategy for DC Power Systems with Constant Power Loads. *IEEE Transactions on Power Electronics*, 23(6), pp. 2982–2989. doi: 10.1109/TPEL.2008.2004594.
- Wu, J. and Lu, Y. (2019). Adaptive Backstepping Sliding Mode Control for Boost Converter With Constant Power Load. *IEEE Access*, 7, pp. 50797–50807. doi: 10.1109/ACCESS.2019.2910936.
- Wu, M. and Lu, D. D. C. (2015). A Novel Stabilization Method of LC Input Filter with Constant Power Loads Without Load Performance Compromise in DC Microgrids. *IEEE Transactions on Industrial Electronics*, 62(7), pp. 4552–4562. doi: 10.1109/TIE.2014.2367005.
- Yousefizadeh, S., Bendtsen, J. D., Vafamand, N., Khooban, M. H., Blaabjerg, F. and Dragičević, T. (2019). Tracking Control for a DC Microgrid Feeding Uncertain Loads in More Electric Aircraft: Adaptive Backstepping Approach. *IEEE Transactions on Industrial Electronics*, 66(7), pp. 5644–5652. doi: 10.1109/TIE.2018.2880666.
- Zhang, Y., Wang, Y., Ni, K. and Hu, Y. (2020). Bidirectional DC–AC Converter-Based Communication Solution for Microgrid. *Power Electronics and Drives*, 5(1), pp. 177–188. doi: 10.2478/pead-2020-0013.
- Zorgani, Y. A., Jouili, M., Koubaa, Y. and Boussak, M. (2019). A Very-Low-Speed Sensorless Control Induction Motor Drive with Online Rotor Resistance Tuning by Using MRAS Scheme. *Power Electronics and Drives*, 4(39), pp. 125–140. doi: 10.2478/pead-2018-0021.